

# Remyelination During Remission in Theiler's Virus Infection

MAURO C. DAL CANTO, MD, and  
RICHARD L. BARBANO, BS

*From the Department of Pathology (Neuropathology), Northwestern University Medical School, Chicago, Illinois*

Inoculation of the cell-adapted WW strain of Theiler's virus into mice produces a chronic demyelinating infection of the central nervous system (CNS) characterized by a remitting relapsing course. During remission, extensive remyelination of spinal cord white matter is observed. Remyelination is carried out by both Schwann cells and oligodendrocytes. This paper examines the possible mechanisms of entry of Schwann cells into the CNS, their possible source in different regions of the white matter, their relations with various CNS elements, and the relative activity of these cells versus that of oligodendrocytes. Observations suggest that Schwann cells, originating from peripheral roots and from perivascular areas, migrate into white matter through gaps in the glial limiting membrane (GLM), probably caused by active mononuclear inflammatory cells. Schwann cell invasion and axonal contact appear to be facilitated by the presence of collagen matrix along their pathway of migration. No alterations of astrocytes in the immediate vicinity of Schwann cells

were observed, and free contact between Schwann cells and different neuroglial elements was present in the initial stages of Schwann cell migration. While Schwann cells were the predominant myelinating cells in the outer white matter, oligodendrocytes were numerous and very active in the inner portions of the spinal cord column. Although oligodendrocytes produced thinner myelin than normal, in most areas essentially complete remyelination by these cells was observed. These results contrast with those of previous studies of DA infected mice in which remyelination is sporadic in the presence of unabated inflammation which continues without remission for many months after infection. It is suggested that oligodendroglial cells are quite capable of extensive remyelinating activity in this infection, provided the noxa responsible for myelin injury subsides. The host inflammatory response appears to be the most likely noxa impeding remyelination in this model. (*Am J Pathol* 1984, 116:30-45)

THEILER'S murine encephalomyelitis virus (TMEV) produces a persistent infection in mice characterized by extensive white matter primary demyelination,<sup>1,2</sup> which appears to be immune-mediated.<sup>3</sup>

Previous studies have shown that mice infected with the DA strain of TMEV develop a chronic paralytic disease characterized by severe unremitting inflammatory demyelination lasting for several months after infection.<sup>2</sup> Remyelination in such mice appears late and is incomplete.<sup>2</sup> Mice infected with the cell-adapted attenuated WW strain of TMEV, on the other hand, develop a remitting relapsing course characterized by extensive remyelination during the periods of remission.<sup>4</sup> We also reported that Schwann cells participated very actively in central nervous system (CNS) myelin repair.<sup>4</sup>

The present study is focused on the first remission in WW infection and sequentially follows the remyelinating activity during this phase of the disease. The

possible source and mode of entry of Schwann cells, their relation to neuroglial cells, and the relative participation of Schwann versus oligodendroglial cells in the process of remyelination will be discussed.

## Materials and Methods

### Virus

WW virus was kindly provided by Dr. Howard Lipton. It was adapted to grow in tissue culture,<sup>5</sup> and a virus stock was prepared on the fourth passage in primary baby mouse kidney cells.

Supported by Grant NS-13011 from the National Institutes of Health.

Accepted for publication January 27, 1984.

Address reprint requests to Mauro C. Dal Canto, MD, Department of Pathology, Northwestern University Medical School, 303 E. Chicago Avenue, Chicago, IL 60611.

## Animals and Inoculations

Outbred Swiss mice (CD-1), purchased from Charles River Laboratories (Portage, Mich) were inoculated intracranially at 4–6 weeks of age with  $10^3$ – $10^4$  plaque-forming units (PFU) of WW virus. Control animals were inoculated with 0.03 ml of minimum essential medium only.

## Tissue Preparation

Animals were anesthetized and perfused with chilled 3% glutaraldehyde in phosphate buffer (pH 7.3). Spinal cord was sectioned at approximately 1 mm intervals, postfixed in 1% osmic acid for 1 hour and processed for Epon embedding. Sections were examined under light and electron microscopy.

## Results

For this study, three time points were selected for examination, 31, 44, and 63 days after infection. Such selection was based on earlier studies, which showed beginning Schwann cell invasion and remyelination at 31 days after infection and complete remyelination at 63 days after infection. Five to seven animals were sacrificed at each time interval.

### Light-Microscopic Studies

#### *Thirty-One Days After Infection*

Rich mononuclear cell infiltrates were present in the subarachnoid space and extended into the Virchow–Robin spaces of the spinal cord (Figure 1). Cells were particularly numerous around the anterior median vessels in the central sulcus and in correspondence with the anterior root exit zone. In the most heavily affected areas, the subpial and perivascular glial limiting membranes (GLMs) were no longer distinguishable amidst the inflammatory cells (Figure 1). In the vicinity of these infiltrates, numerous demyelinated axons were present. Frequently at the level of the root exit zone, demyelination of the central portion of the root fibers was observed, while the peripheral portion appeared unremarkable (Figure 2). In most sections, areas around the central sulcus and the anterior root exit zone showed considerable vascular activity. Numerous spindle cells were closely associated with the larger vessels whose walls appeared moderately thickened. In continuity with these vessels numerous septa criss-crossed the surrounding white matter, imparting to it a lobular architecture. Among the cells present in these septa, Schwann cells

could easily be recognized in many sections (Figures 3 and 4).

#### *Forty-Four Days After Infection*

At this stage, large groups of axons were remyelinated by Schwann cells in the vicinity of the anterior root and anterior paramedian areas of the spinal cord (Figures 5 and 6). Whereas in some sections the intervening white matter was free of Schwann cells, in others it began to show peripheral-type myelin in close association with numerous middle-sized vessels in the area. Lack of Schwann cells in the superficial layers of the spinal cord at these levels (Figure 7) suggested *in situ* perivascular proliferation of Schwann cells rather than downward migration from the overlying subarachnoid space. Axons surrounded by peripheral-type myelin were readily recognizable because of their thick myelin sheaths and a one-to-one relationship with their respective myelinating cells (Figure 6).

In the inner half of the spinal cord most axons were surrounded by very thin myelin sheaths, consistent with an oligodendroglial origin (Figure 7). In most spinal cords remyelinating activity by oligodendroglial cells appeared to lag behind that of Schwann cells in adjacent areas of the same sections.

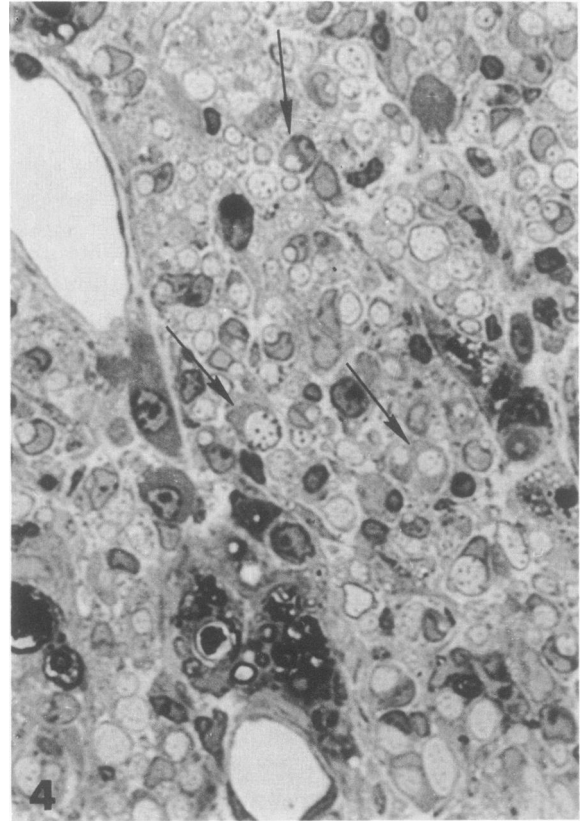
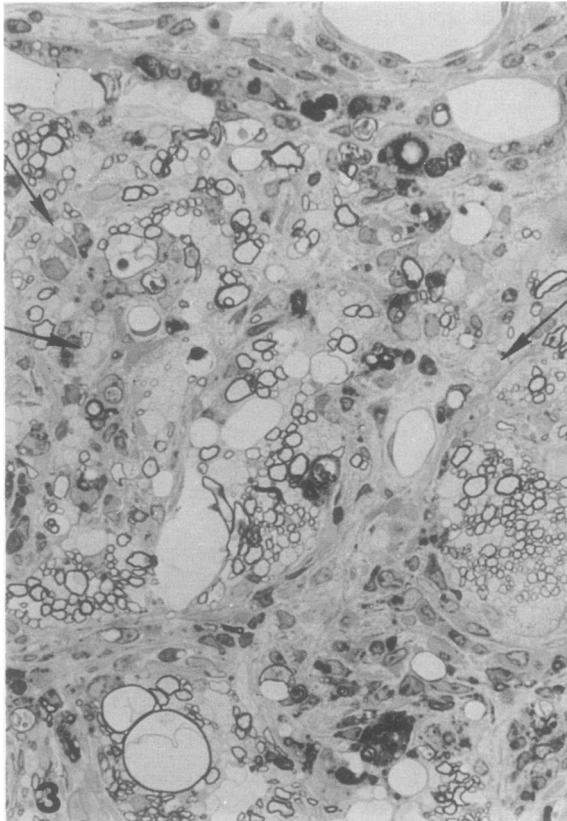
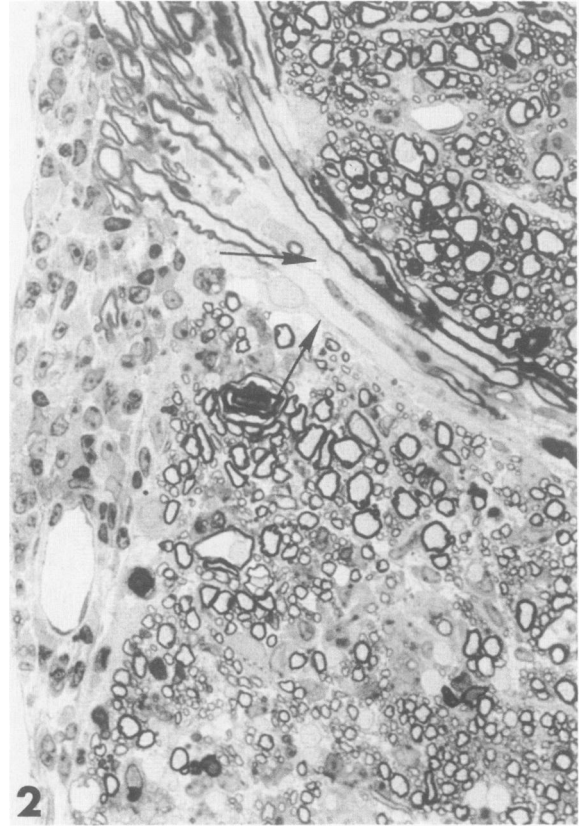
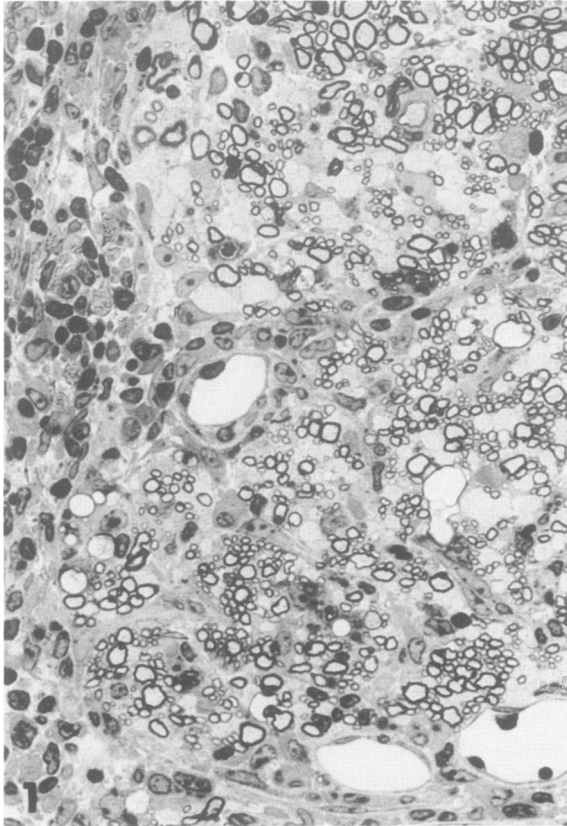
#### *Sixty-Three Days After Infection*

At this later stage, the outer superficial white matter between the root and the median sulcus was heavily populated by Schwann cells. Most sections therefore showed an uninterrupted layer of peripheral-type myelin in the entire outer half of the anterior and lateral columns (Figure 8). The inner half of the white matter, on the other hand, was entirely remyelinated with thin myelin sheaths of apparent oligodendroglial origin. At the border between peripheral and central-type myelin, Schwann-cell-associated axons were interdigitating with thinly sheathed axons along a rather narrow transition line. At this stage, inflammatory activity was largely absent (Figure 8).

### Ultrastructural Studies

#### *Thirty-One Days After Infection*

At this time, inflammatory infiltrates mainly consisted of lymphoid cells, but several mature plasma cells were already present. Macrophages rich in myelin debris were abundant in the midst of demyelinated axons. Interestingly, the plasma membrane of macrophages often showed coated pits, and their cytoplasm was rich in myelin-containing phagosomes when in the vicinity of degenerating myelin, as also



described in other primary demyelinating conditions (Figure 9).<sup>6,7</sup>

An important change consisted in the alteration of the GLM at the sites of maximal inflammatory activity. Both basement membrane and glial foot processes showed variable degrees of injury which eventually resulted in segmental interruptions of the GLM at both pial and perivascular levels (Figures 10 and 11). Since most severe mononuclear infiltrates were following perforating vessels of larger diameter, lesions of the GLM were most severe at the surface of the spinal cord and around vessels in the outer half of the anterior and lateral columns. Numerous Schwann cells were observed penetrating through gaps of the GLM in these locations (Figures 10 and 11). In this initial stage of invasion, penetrating Schwann cells came into close contact with preexisting CNS elements, ie, astrocytes and oligodendroglial cells (Figures 12 and 13). The only structure separating peripheral from central elements was at this time the basement membrane of the invading cells. No morphologic alterations were present in either astrocytes or oligodendrocytes while Schwann cell penetration was taking place (Figures 12 and 13).

Morphologic changes around vessels were of particular interest for the role they played in Schwann cell colonization of areas at a distance from the roots, especially the paramedian zone. In agreement with light-microscopic observations, numerous cellular profiles were present in the perivascular spaces. These profiles consisted of inflammatory cells, fibroblasts, and Schwann cells, the latter being surrounded by a basement membrane (Figure 14). A few of the Schwann cell profiles appeared noncommitted at this time, but most had made contact with naked axons, and myelin was already being formed around those of larger diameter (Figure 14). Numerous collagen fibers were present among the cells.

Deeper in between vessels, demyelinated axons were grouped in lobular aggregates, which were separated by long slender cells consistent with fibroblasts, and by collagen fibers (Figure 15). Where interlobular collagen contacted the surface of the lobular aggregates, a discontinuous basement-membrane-like structure

was generally produced around the lobules. Fibroblasts and collagen fibers had clearly extended from the perivascular spaces and appeared to form a scaffolding that Schwann cells followed to penetrate into the spinal cord. By this route, Schwann cells extended into the interlobular spaces and reached the surface of the lobular aggregates (Figure 16).

Schwann cell entry into the lobules was accomplished either through discontinuities in the external lobular basement membrane or by fusion of such membrane with the basement membrane of the Schwann cells (Figures 16 and 17). Upon entry, Schwann cells extended their processes around demyelinated axons, starting from the most superficial and proceeding toward the center of the lobule. In this fashion, entire lobules were eventually invaded by Schwann cells (Figure 18). Interestingly, astrocytic processes failed to show significant changes during this phase of Schwann cell invasion.

#### *Forty-Four Days After Infection*

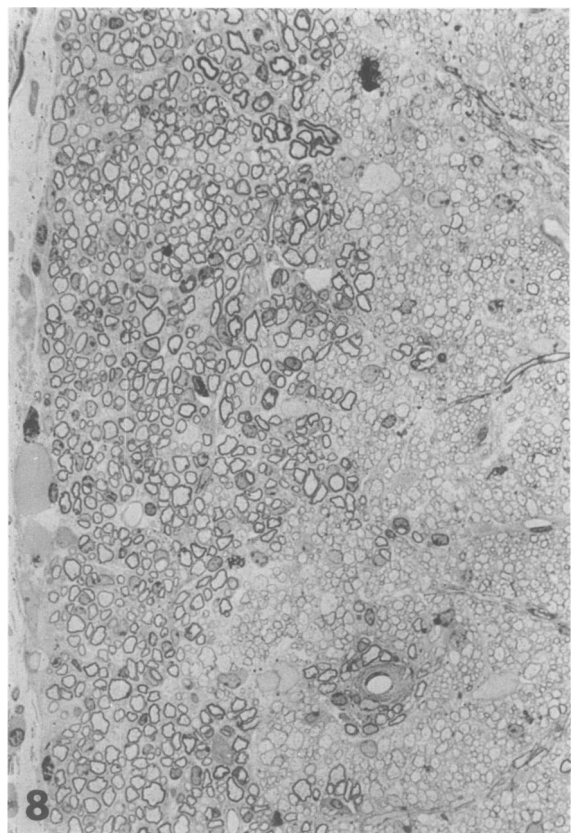
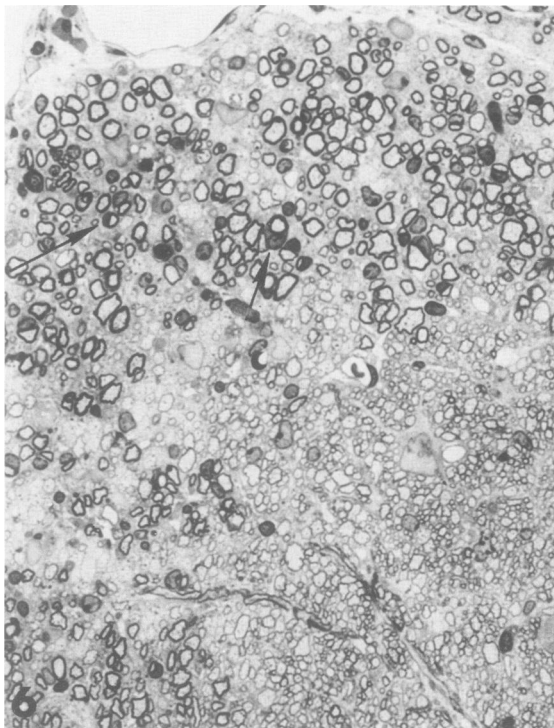
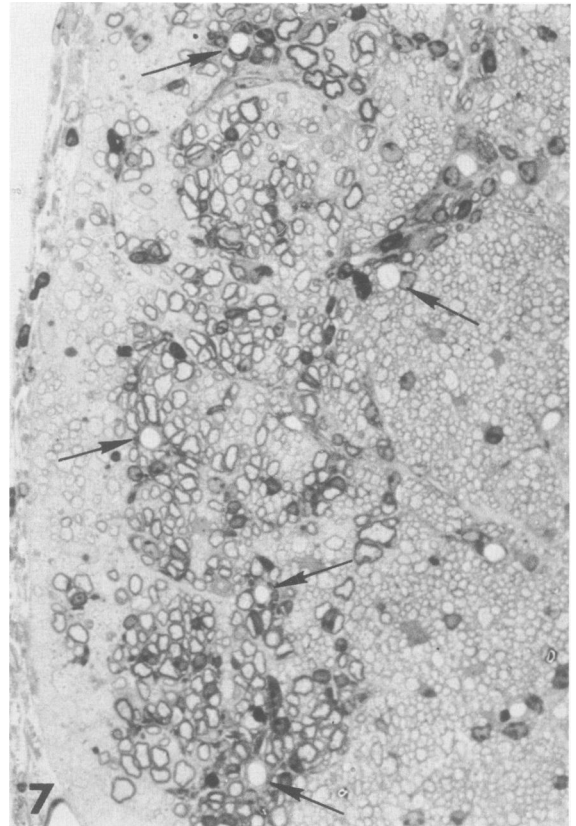
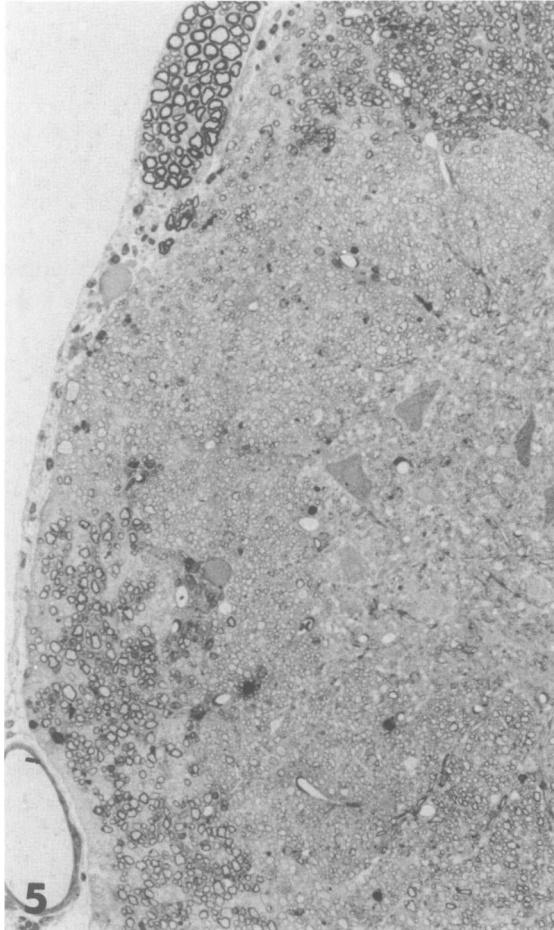
At this time, there was a significant decrease in the inflammatory component, and the GLM showed evidence of repair, both at the pial surface and around blood vessels. A newly reconstituted GLM was characterized by one to several layers of glial processes covered by a basement membrane (Figure 19). At this stage of the disease, Schwann cell activity had largely subsided, because complete remyelination of the invaded areas had been reached. Further Schwann cell migration was probably inhibited by the repair of the GLM (Figure 19). The remyelinated areas still preserved a lobular pattern due to the presence of rather thick collagen septa.

Oligodendroglial cell activity had also peaked at this time interval. Demyelinated areas in the inner half of spinal cord white matter were being actively remyelinated by oligodendrocytes (Figures 20 and 21). Where oligodendroglial cells and Schwann cells came into competition, they seemed to intermingle freely without interfering with each other. Axons appeared to be remyelinated by the cell which happened to contact them first (Figure 20).

The pattern of myelination by oligodendroglial

Figures 1 through 8 are of 1- $\mu$ -thick Epon-embedded sections stained with toluidine blue. **Figure 1**—Numerous mononuclear inflammatory cells are present in the leptomeninges (*left*) and around blood vessels (*center and bottom*). Groups of naked axons are present in the vicinity of the inflammatory infiltrates. Disorganization of the GLM is best appreciated in the upper portion of the photograph. (31 days after infection,  $\times 380$ ) **Figure 2**—Leptomeninges (*left*) are rich in mononuclear inflammatory cells at the level of the anterior root exit zone. Several fibers constituting the central portion of the root are demyelinated (*arrows*), while the peripheral portion is not. Some central demyelinated axons are also visible at the bottom of the picture. (31 days after infection,  $\times 410$ ) **Figure 3**—Streaming of inflammatory and spindly cells from perivascular areas produces a lobular architecture in the white matter of this anterior column. Meninges and large meningeal vessels are at the top of the photograph. There are numerous demyelinated axons, and some have already been contacted by Schwann cells (*arrows*). (31 days after infection,  $\times 380$ ) **Figure 4**—An area of white matter around the central sulcus shows in greater detail how numerous demyelinated axons have been surrounded by Schwann cells (*arrows*). (31 days after infection,  $\times 600$ )





cells was identical to that observed in the developing animal. A few instances of abnormal cell-membrane-axon attachments and redundant myelin loops were observed, but they are also known to occur during normal myelination and remodeling. In the transition areas, where axons were shared equally by Schwann cells and oligodendrocytes, a GLM-like structure was eventually formed separating the central elements from the peripheral (Figure 22). This arrangement simulated the anatomic appearance of normal CNS-PNS junctions. Very little gliosis was noted in the centrally remyelinated areas.

#### *Sixty-Three Days After Infection*

This time point was essentially characterized by very little remaining inflammation and by essentially total remyelination along the entire spinal cord with prevalently Schwann cells in the outer half and oligodendrocytes in the inner half of the anterior and lateral columns. At this stage, a few aberrant myelinated axons were also observed in the subarachnoid space along the anterior rim of the spinal cord. Such axons had never been seen at earlier times, and were much less numerous than reported in chronic relapsing EAE.

### Discussion

This study has shown that during remission in the WW model of Theiler's virus infection remyelination of spinal cord white matter is essentially complete. Both Schwann and oligodendroglial cells participate in the process of myelin repair, but important differences in their respective activities are noted.

Schwann cell invasion and remyelination of CNS white matter were dependent on previous events leading to injury of the GLM. Morphologically, such injury was mainly localized at sites of maximal inflammatory infiltration, ie, around the anterior roots and around vessels in the anterior central sulcus. Schwann cells were observed penetrating through gaps in the GLM at these two locations and subsequently making contact with demyelinated central axons.

Blakemore et al<sup>8</sup> have previously stressed the im-



**Figure 9**—This macrophage is stripping myelin (*top*) from an axon. Myelin fragments are enclosed in autophagic vacuoles (*arrow*). (31 days after infection,  $\times 30,800$ )

portance of the GLM as a barrier to the penetration of Schwann cells into the spinal cord. In experiments leading to destruction of the GLM with X-irradiation<sup>9</sup> or toxic agents, such as lysolecithin<sup>8</sup> or 6-amino-nicotinamide,<sup>10</sup> injury of the GLM always preceded CNS invasion and remyelination by Schwann cells. Focal remyelination of spinal cord by Schwann cells has also been observed in chronic EAE<sup>7</sup> and in human multiple sclerosis (MS) as well.<sup>11</sup> In such diseases, however, the role of inflammation in the production of GLM injury has not been specifically addressed. The present study strongly suggests that infiltrating inflammatory cells play a major role in the destruction of the GLM, although the basic mech-

**Figure 5**—The areas adjacent to the anterior root (*top*) and that adjacent to the central sulcus (*bottom*) contain numerous axons surrounded by peripheral type myelin and Schwann cells. Axons in the remaining white matter are either naked or surrounded by thinner myelin characteristic of an oligodendroglial origin. (44 days after infection,  $\times 120$ ) **Figure 6**—The central sulcus is at the *top* of the picture. The adjacent area has been remyelinated by Schwann cells, most of which at this magnification are easily identifiable (*arrows*). Thinner myelin in the lower right-hand side of the photograph is of oligodendroglial origin. (44 days after infection,  $\times 400$ ) **Figure 7**—Numerous middle-sized vessels (*arrows*) are surrounded by groups of Schwann-cell-remyelinated axons in this section from the anterolateral column. Note how the submeningeal area (*left*) is free of Schwann cells, suggesting their migration from local vessels rather than from meningeal space. (44 days after infection,  $\times 400$ ) **Figure 8**—The entire thickness of the outer half of the anterior and lateral column is mainly remyelinated by Schwann cells, while the inner half is surrounded by thinner central-type myelin. (63 days after infection,  $\times 280$ )

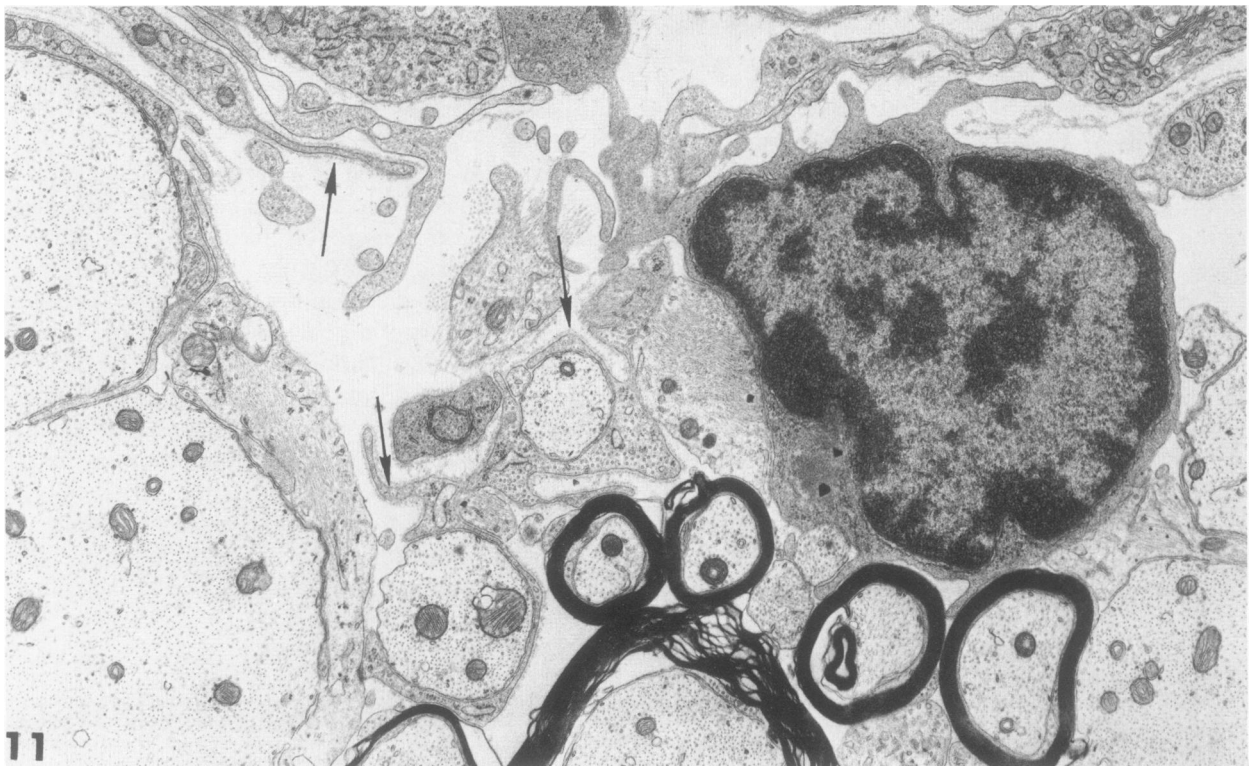
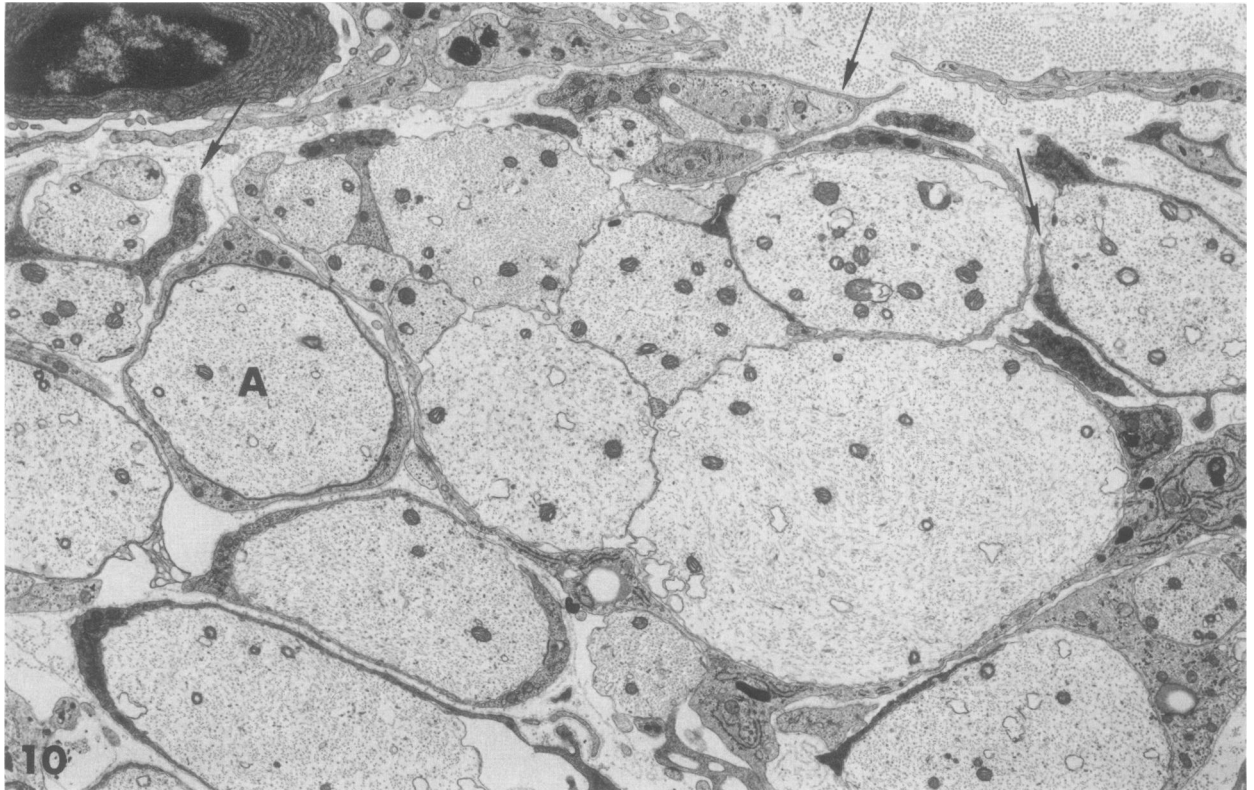


**Figure 10**—A plasma cell is seen in the meninges from an area close to an anterior root. There is complete disappearance of the GLM, resulting in the exposure of naked axons to elements in the subarachnoid space. Numerous Schwann cell processes (*arrows*) are seen penetrating between the axons and surrounding the largest ones. The beginning of myelin formation is present around the axon marked A. (31 days after infection,  $\times 12,000$ ) **Figure 11**—The GLM cannot be recognized at the surface of the white matter abutting on this perivascular space. A lymphoid cell and numerous other mononuclear cell profiles are present in the disorganized area, together with infiltrating Schwann cells (*arrows*). (31 days after infection,  $\times 20,000$ )



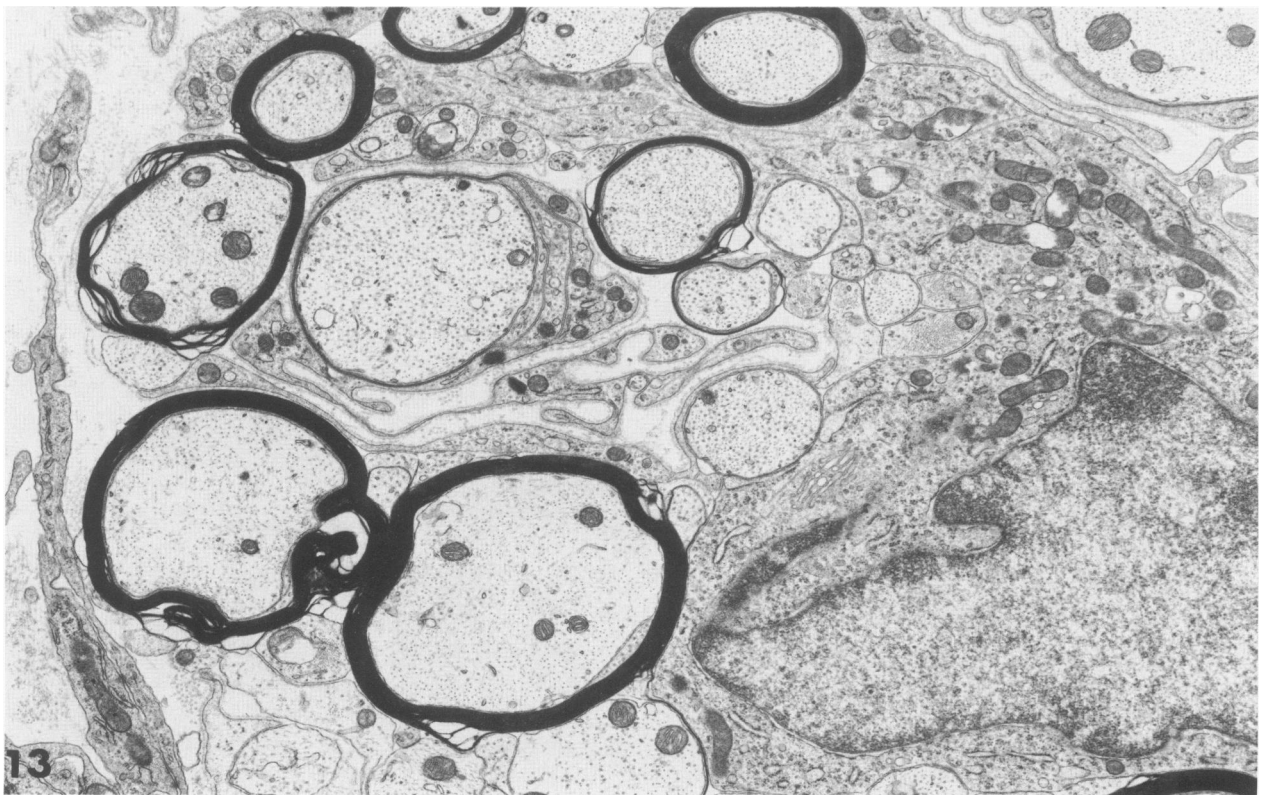
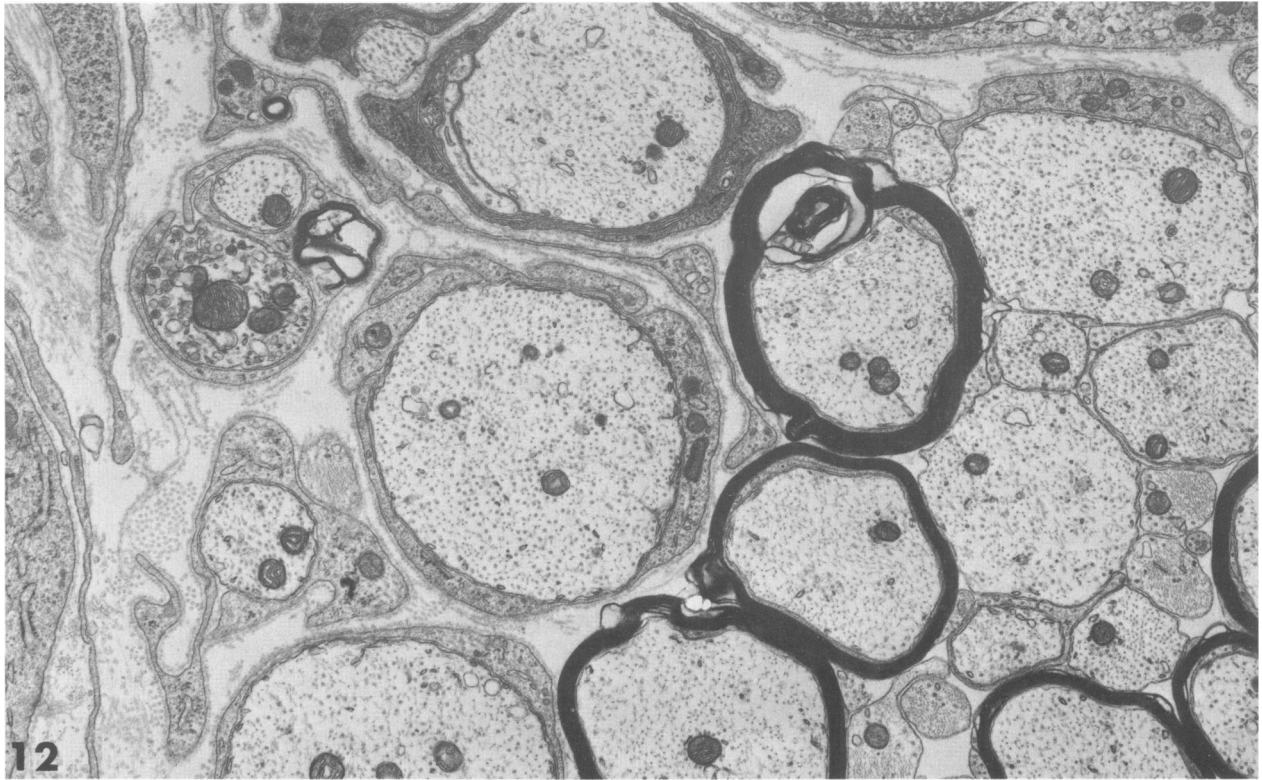


**Figure 12**—Numerous Schwann cells are penetrating the spinal cord from a perivascular space. No separation other than by Schwann cell basement membrane is present between Schwann cells, naked axons, and other structures such as central myelin and astrocytic processes. (31 days after infection,  $\times 12,800$ ) **Figure 13**—The lack of a GLM has allowed penetration of Schwann cells into the surface of the anterior column. A large oligodendroglial cell (*right*) in the immediate vicinity appears normal. Numerous naked axons are present. (31 days after infection,  $\times 10,000$ )

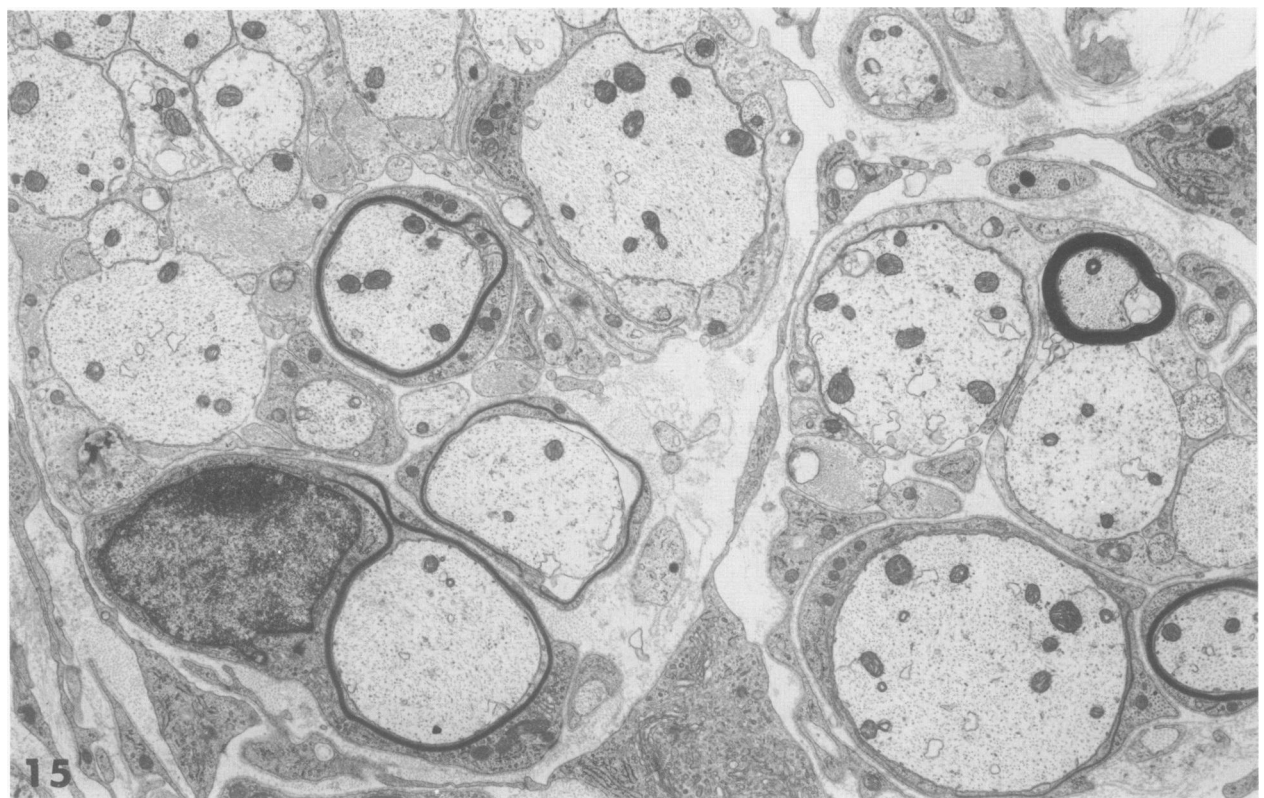
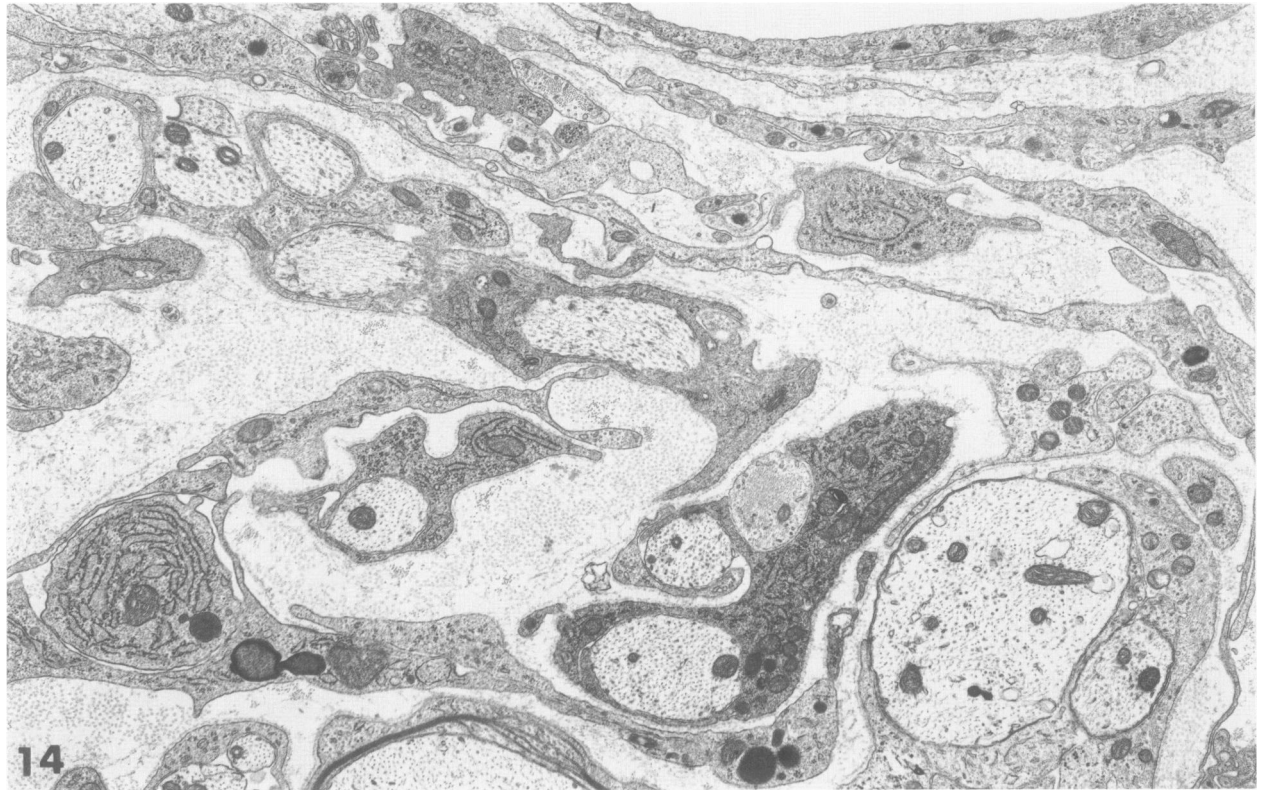


**Figure 14**—Perivascular space shows numerous Schwann cell profiles, most of which have contacted demyelinated axons. Note the absence of a GLM, abundant collagen fibers, and myelin formation around the two largest axons at the bottom and lower right-hand corner of the photograph. (31 days after infection,  $\times 11,000$ ) **Figure 15**—Large lobular aggregates of demyelinated axons separated by slender cells and collagen fibers are seen. Note how Schwann cells take over each lobule, starting from the most superficial axons. Myelin is beginning to form around some of the largest axons. (31 days after infection,  $\times 9500$ )

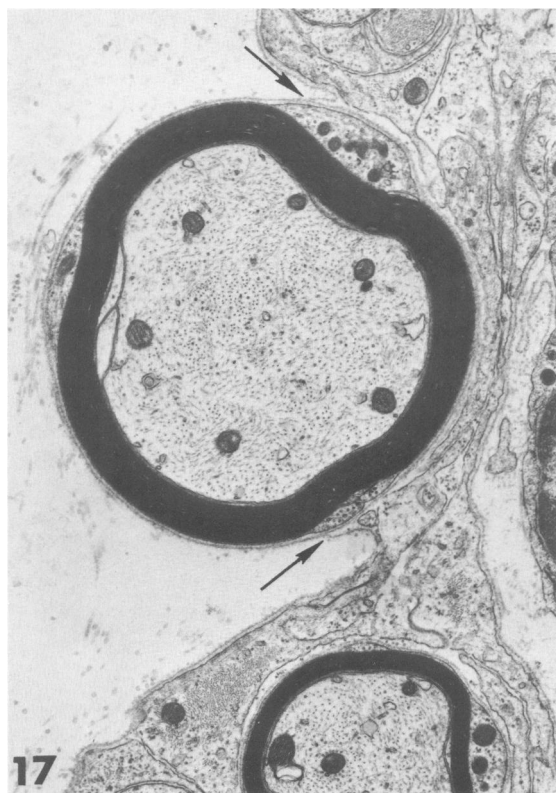
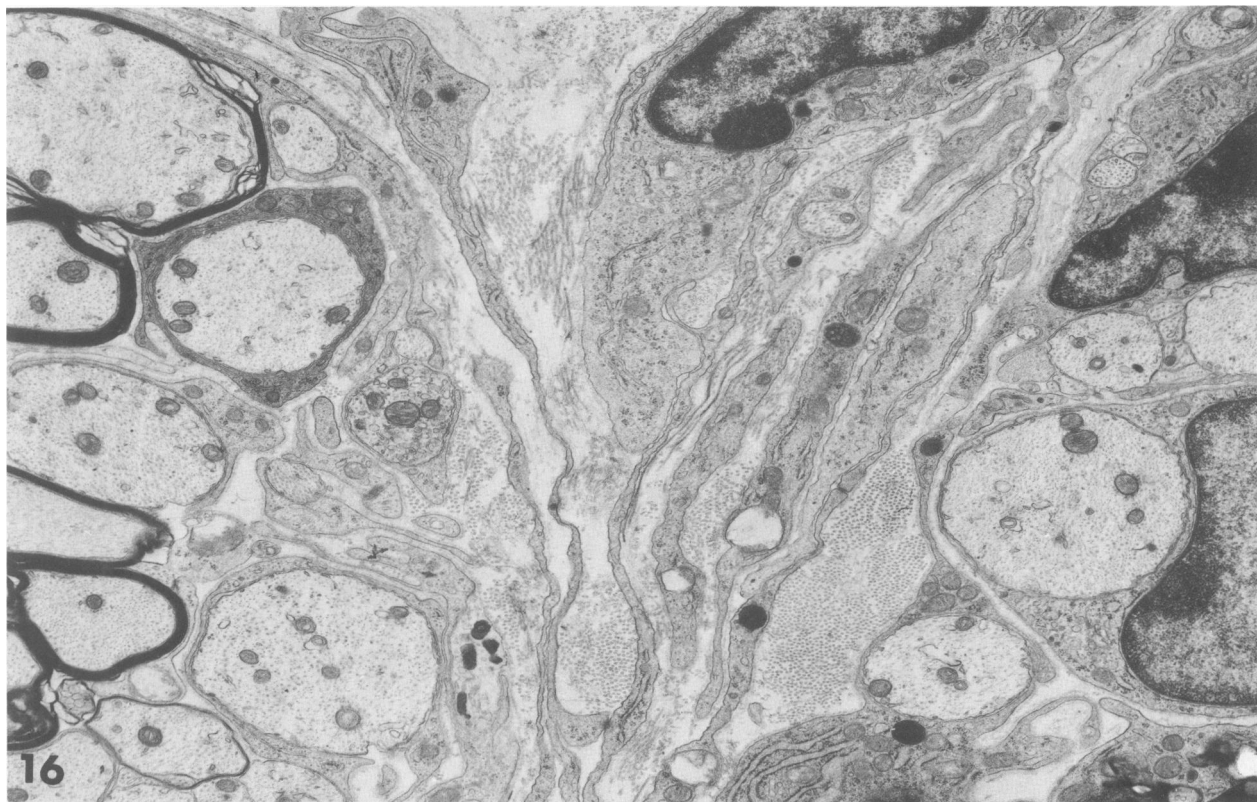


**Figure 16** – The central area of this photograph shows abundant collagen and fibroblasts, among which Schwann cells stream down from a perivascular space in between lobular aggregates of naked axons. The outermost axons from each aggregate have been captured by Schwann cells. (31 days after infection,  $\times 10,000$ ) **Figure 17** – Arrows point at the fusion between a Schwann cell basement membrane and the basement membrane which is present on the surface of one of the lobular aggregates. (31 days after infection,  $\times 14,400$ )



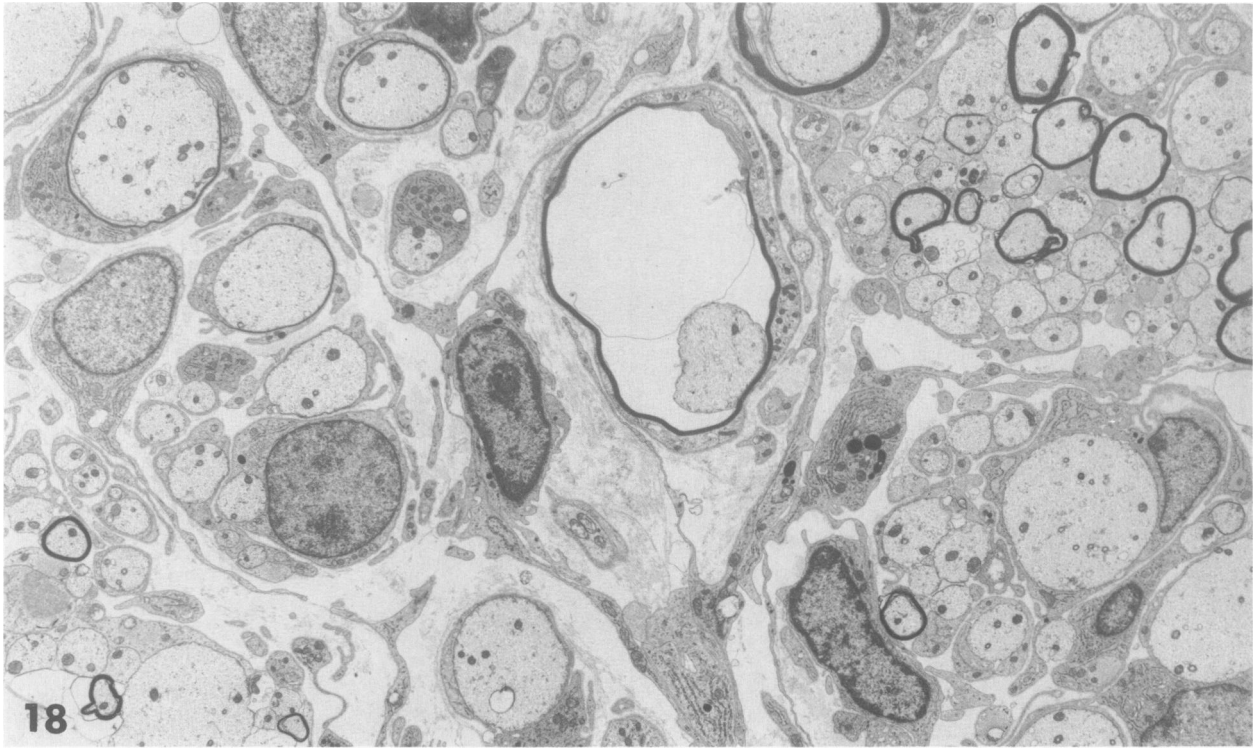


**Figure 18**—All lobular aggregates of naked axons except the one in the upper right-hand corner of the photograph have been completely repopulated by Schwann cells. (31 days after infection,  $\times 8000$ ) **Figure 19**—Reconstitution of a GLM is seen at the surface of the spinal cord. The GLM is now made of multiple interdigitating layers of astrocytic processes and basement membrane. The myelin in this picture is all of the peripheral type, and Schwann cells are clearly recognizable. (44 days after infection,  $\times 14,000$ )

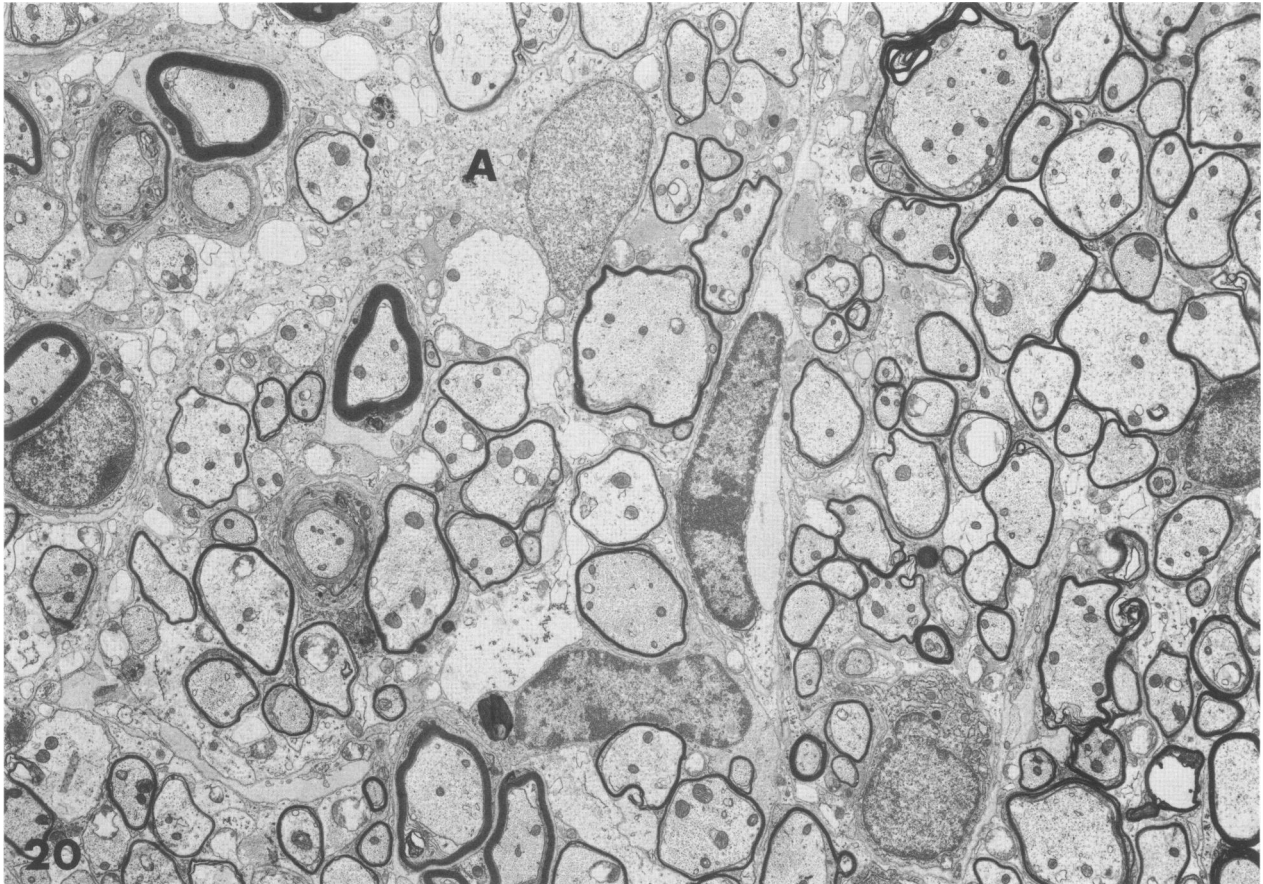


**Figure 20**— This low-magnification photograph shows the transition area between peripheral-type remyelination (*left*) and central-type remyelination (*most of center and right*). There is free interdigitation of central and peripheral elements in a jigsaw pattern. An astrocyte (A) sends its processes between Schwann-cell-remyelinated axons. (44 days after infection,  $\times 2500$ )

anisms are open to speculation. Both physical disruption and biochemical alterations seem possible, but recent studies would support the latter alternative as the most likely. It is known, for instance, that metalloproteinases secreted by macrophages and endothelial cells may degrade Type IV and Type V collagens, which are the structural components of basement membranes.<sup>12,13</sup> In addition, lymphokines have long been known to produce nonspecific tissue injury during inflammation. A direct relation between inflammation and GLM injury correlates with the observation of maximal Schwann cell invasion in areas presenting the most severe inflammatory infiltrates.

The source of Schwann cells was mainly dependent on anatomic factors. At the level of the anterior roots, the major source of Schwann cells was most likely the adjacent peripheral fibers. Both at light microscopy and ultrastructurally, demyelination of the central component of the anterior root fibers was clearly observed at most levels. Schwann cells on the peripheral component of these fibers thus came in contact with the naked central portion upon destruction of the

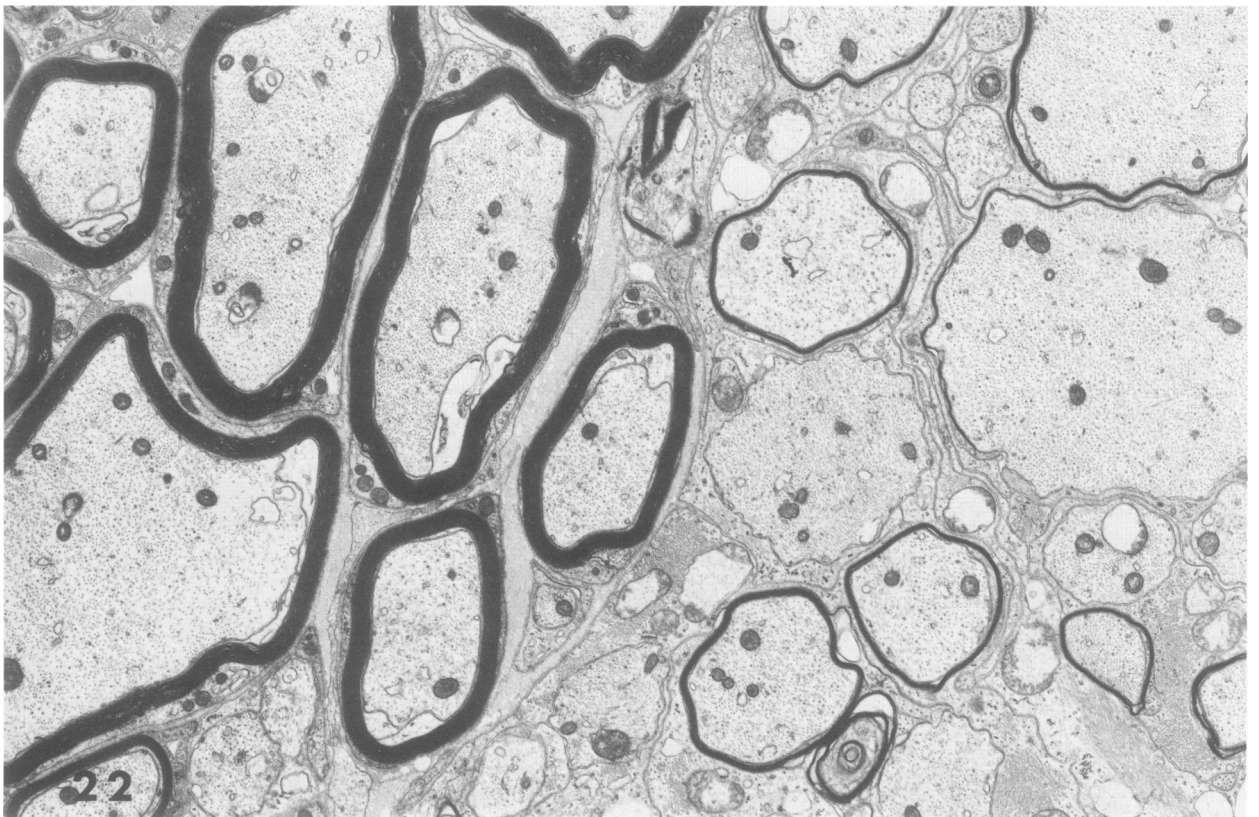
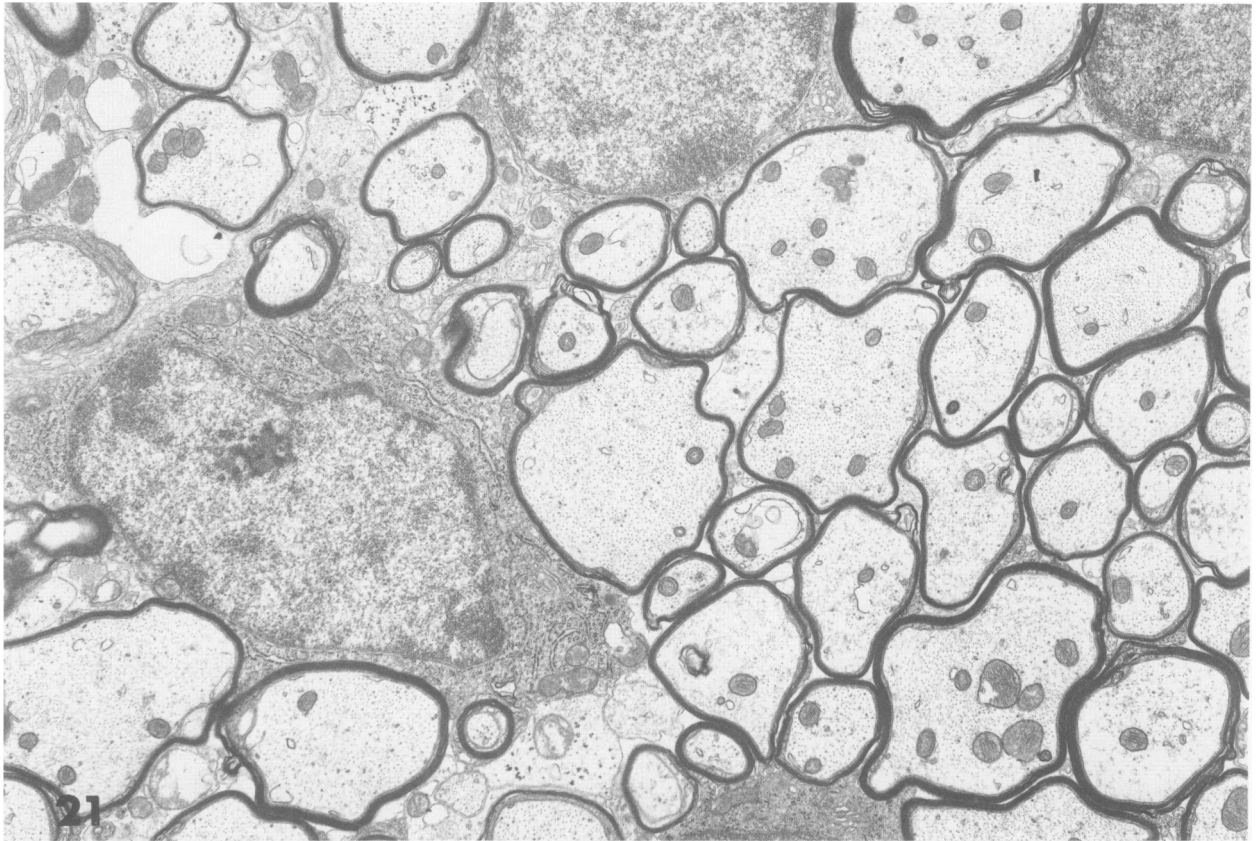
GLM by the inflammatory cells. It is well known that Schwann cells are stimulated into proliferation and myelin synthesis in the presence of naked axonal membranes.<sup>14</sup>

The source of Schwann cells at the level of the anterior median sulcus is more difficult to explain.

It seems unlikely that these cells migrated from the anterior roots, because initially Schwann cells were not present in the wide zone enclosed between the anterior roots and the central sulcus, whereas both these areas were already richly provided with Schwann cells, as shown in Figure 5.

Another unlikely source of CNS peripheral-type myelin would be the rare foci of Schwann cells which have been described in normal spinal cord.<sup>15</sup> The amount of Schwann cell remyelination in our study is in fact too great and too consistent to be explainable on that basis.

A third possibility, suggested by others, in chronic EAE,<sup>16</sup> is that of Schwann cell origin from aberrant sensory axons in the subarachnoid space. This is also unlikely in our model, because no such aberrant



axons were seen during the peak of Schwann cell activity, and rare isolated peripheral axons were not present in the subarachnoid space until the last time interval of this study.

A fourth possibility is that of an origin from Schwann cells surrounding autonomic nerves in contact with the larger meningeal and perforating vessels. The presence of a vascular innervation in the CNS has long been debated. Recently, morphologic and histochemical studies have shown that in several species, from reptiles to mammals, arteries, arterioles and in some species, capillaries are indeed endowed with rich autonomic innervation.<sup>17-20</sup> Several points would support such an origin in our study: 1) the spinal central sulcus does contain the largest spinal cord vessels; 2) Schwann cell invasion is limited to the outer portion of the white matter, where the largest perforators are found; 3) both light-microscopic and ultrastructural examinations show that most Schwann cells are localized in perivascular position before migrating into the spinal cord parenchyma.

Migration of Schwann cells from their sites of entry into the spinal cord parenchyma appeared to be facilitated by fibroblastic proliferation and collagen deposition, which were especially prominent around vessels in response to inflammation. It was apparent that Schwann cells followed fibroblast and collagen fibers into the spinal cord white matter in order to make contact with the lobular aggregates of demyelinated axons. The presence of collagen should be especially recognized as an important factor leading to the successful interaction between Schwann cells and axons. Bunge et al demonstrated that Schwann cells could not complete their differentiation and interact normally with axons unless provided with a connective tissue matrix which would constitute the secondary or permissive inductive signal for the full expression of cell function.<sup>21</sup> Our results support this interpretation by clearly showing a constant interaction between Schwann cells and the collagen substrate before axonal cell contact and myelin production.

During the course of the infection, invading Schwann cells and astrocytes showed interesting changes in their relations. As Schwann cells were advancing into the lobular aggregates of naked axons, astrocytic processes were simply displaced aside but did not show any morphologic alterations of the type

described in the model of X-irradiation by Blake-more.<sup>22</sup> Initially astrocytic processes facing advancing Schwann cells appeared naked. At later stages, on the other hand, a continuous limiting membrane was observed interposed between astrocytes and the basement membrane of Schwann cells. Such an arrangement recapitulated the normal relationship between Schwann cells and astrocytes at the level of the peripheral roots.

An important finding in this study was the degree of oligodendroglial participation in the remyelination of spinal cord lesions. For many years, oligodendroglial cells were thought to be incapable of remyelinating demyelinated axons to any significant degree. Recently, a number of investigations have demonstrated that remyelination by oligodendroglial cells is possible, and the ability of oligodendrocytes to undergo proliferation in the adult animal has been proven in several experimental models.<sup>7,23,24</sup> Remyelination by oligodendrocytes has also been demonstrated in human MS, albeit in a sporadic, unpredictable fashion. For instance, some of the shadow plaques, previously thought to represent incomplete demyelination, have been shown to contain numerous remyelinated axons.<sup>25</sup>

Infection with the cell-derived attenuated WW strain of TMEV is characterized by an extraordinary degree of oligodendroglial cell remyelination, which contrasts with that previously observed in mice infected with the brain-derived DA strain of TMEV in which myelin repair is in many ways similar to that in human MS, focal and unpredictable.<sup>22</sup>

Possible reasons for different remyelinating activity following infection with the two viral strains could be the following: 1) a different viral tropism for oligodendrocytes, 2) a different astroglial response in the two infections producing different degrees of scarring, 3) a different temporal development and degree of severity of the inflammatory response to the two strains.

Morphologically and by immunohistochemistry, there is no appreciable difference in the degree of oligodendroglial injury between infection by DA and WW strains of TMEV.<sup>26,27</sup> In both cases, viral presence in these cells is sporadic, and it is only appreciated when demyelination has been already well under way.<sup>26-28</sup> The role, if any, that viral infection of oligo-

← **Figure 21**—Four oligodendroglial cells are present in this field, together with many remyelinated axons. Myelin is thinner than normal, but essentially all axons have been remyelinated. Oligodendrocytes appear as normal mature cells. (44 days after infection, × 8000) **Figure 22**—Clear separation between the group of axons remyelinated by Schwann cells (*left*) and the group of axons myelinated by oligodendrocytes (*right*) recapitulates the normal appearance at the root-entry zones. (44 days after infection, × 11,000)



dendrocytes may have in myelin degeneration in Theiler's infection is therefore still controversial.

The possible adverse effect that astroglial scarring may have on the process of oligodendroglial-axon contact and remyelination is still open to debate. Most investigators think that such a role is probably not significant. Bunge et al, stress the fact that remyelination is seen in the cerebrospinal fluid barbotage lesion, where astrocytic scarring is present.<sup>21</sup> Ludwin also discards the possibility of mechanical interference to remyelination by astrocytic processes, because no appreciable difference in scarring was present between the acute and chronic models of cuprizone toxicity, while remyelination was much more prominent in the acute model.<sup>29</sup> In our system, obvious differences in the severity of the astrocytic response were present, but only after many months of infection. If we consider a relatively recent time point, ie, around 2 months after infection, no appreciable difference in scarring was present between the two infections, yet remyelination was practically complete in the WW model and only sporadic in the DA model. These findings would thus support the contention that astroglial reaction has probably little role in the outcome of the remyelinating process.

The most obvious difference between the two infections was in the severity of the inflammatory response and in the temporal development of the disease. In the DA model, inflammation continues unabated for several months after infection and is severe even at 7 months after inoculation.<sup>2</sup> No evidence of remission, either clinically or pathologically, is observed, and remyelination as seen in previous studies is focal and only appears several months after infection.<sup>2</sup> In contrast, mice infected with the attenuated WW strain show a milder degree of inflammation and most importantly a remitting relapsing course.<sup>4</sup> During the first remission, between 5 and 8 weeks after infection, inflammation decreases to minimal levels, while at the same time remyelinating activity steadily increases. It thus appears that successful remyelination in this model is strongly dependent on the abatement of the inflammatory response. In this respect, this model of virus-induced demyelination parallels demyelinating models produced by physical or chemical injury in which remyelination also appears to take place when the offending noxa either subsides or is removed. Mechanisms underlying remission and relapses in Theiler's infection appear to depend on the host immune response, because viral titers are on a steady plateau for several months,<sup>5</sup> and viral antigen can be visualized by immunocytochemistry for the entire period of the infection.<sup>27</sup>

This study suggests that oligodendroglial cells are

not the limiting factor in the process of remyelination. Oligodendrocytes and Schwann cells, if available, are quite capable of remyelinating extensive areas of CNS provided the noxa responsible for myelin injury subsides. In Theiler's infection, such a noxa is most probably represented by the host antiviral inflammatory response.

## References

1. Lipton HL: Theiler's virus infection in mice: an unusual biphasic disease process leading to demyelination. *Infect Immun* 1975, 11:1147-1155
2. Dal Canto MC, Lipton HL: Primary demyelination in Theiler's virus infection: An ultrastructural study. *Lab Invest* 1975, 33:626-637
3. Lipton HL, Dal Canto MC: Theiler's virus-induced demyelination: Prevention by immunosuppression. *Science* 1976, 192:62-64
4. Dal Canto MC, Lipton HL: Schwann cell remyelination and recurrent demyelination in the central nervous system of mice infected with attenuated Theiler's virus. *Am J Pathol* 1980, 98:101-122
5. Lipton HL, Dal Canto MC: The TO strains of Theiler's viruses cause "slow virus-like" infection in mice. *Ann Neurol* 1979, 6:25-28
6. Prineas JW, Connell F: The fine structure of chronically active multiple sclerosis plaques. *Neurology* 1978, 28:68-75
7. Raine CS: Multiple sclerosis and chronic relapsing EAE: Comparative ultrastructural neuropathology. In *Multiple Sclerosis*. Edited by JF Hallpike, CWM Adams, WW Tourtellotte. Baltimore, Williams and Wilkins, 1983, pp 413-460
8. Blakemore WF: Invasion of Schwann cells into the spinal cord of the rat following local injection of lysolecithin. *Neuropathol Appl Neurobiol* 1976, 2:21-39
9. Gilmore SA, Duncan D: On the presence of peripheral-like nervous and connective tissue within irradiated spinal cord. *Anat Rec* 1968, 160:675-690
10. Blakemore WF: Remyelination by Schwann cells of axons demyelinated by intraspinal injection of 6-aminocotinamide in the rat. *J Neurocytol* 1975, 4: 745-757
11. Ghatak NR, Hirano A, Doron Y, Zimmermann HM: Remyelination in multiple sclerosis with peripheral type myelin. *Arch Neurol* 1973, 29:262-267
12. Mainardi CL, Seyer JM, Kang AH: Type-specific collagenolysis: A type V collagen-degrading enzyme from macrophages. *Biochem Biophys Res Commun* 1980, 97:1108-1115
13. Kalebic T, Garbisa S, Glaser B, Liotta LA: Basement membrane collagen: Degradation by migrating endothelial cells. *Science* 1983, 221:281-283
14. DeVries GH, Salzer JL, Bunge RP: Axolemma-enriched fractions isolated from PNS and CNS are mitogenic for cultured Schwann cells. *Dev Brain Res* 1982, 3:295-299
15. Raine CS: On the occurrence of Schwann cells in the normal central nervous system. *J Neurocytol* 1976, 5: 371-380
16. Raine CS, Brown AM, McFarlin DE: Heterotopic regeneration of peripheral nerve fibers into the subarachnoid space. *J Neurocytol* 1982, 11:109-118
17. Nelson E, Takayanagi T, Rennels ML, Kawamura J: The innervation of human intracranial arteries: A study by scanning and transmission electron microscopy. *J Neuropathol Exp Neurol* 1972, 31:526-534

18. Iijima T, Wasano T, Tagawa T, Ando K: A histochemical study of the innervation of cerebral blood vessels in the snake. *Cell Tissue Res* 1977, 179:143-155
19. Tagawa T, Ando K, Wasano T: A histochemical study of the innervation of the cerebral blood vessels in the domestic fowl. *Cell Tissue Res* 1979, 198:43-51
20. Ando K: A histochemical study on the innervation of the cerebral blood vessels in bats. *Cell Tissue Res* 1981, 217:55-64
21. Bunge RP, Bunge M, Cochran M: Some factors influencing the proliferation and differentiation of myelin-forming cells. *Neurology* 1978, 28:59-67
22. Blakemore WF, Patterson RC: Observations on the interrelation of Schwann cells and astrocytes following x-irradiation of neonatal rat spinal cord. *J Neurocytol* 1975, 4:573-585
23. Herndon RM, Price DP, Weiner LP: Regeneration of oligodendroglia during recovery from demyelinating disease. *Science* 1977, 195:693-694
24. Ludwin SK: An autoradiographic study of cellular proliferation in remyelination of the central nervous system. *Am J Pathol* 1979, 95:683-696
25. Prineas JW, Connell F: Remyelination in multiple sclerosis. *Ann Neurol* 1979, 5:22-31
26. Dal Canto MC, Lipton HL: Ultrastructural immunohistochemical localization of virus in acute and chronic demyelinating Theiler's virus infection. *Am J Pathol* 1982, 106:20-29
27. Dal Canto MC: Uncoupled relationship between demyelination and primary infection of myelinating cells in Theiler's virus encephalomyelitis. *Infect Immun* 1982, 35:1133-1138
28. Rodriguez M, Leibowitz JL, Lampert PW: Persistent infection of oligodendrocytes in Theiler's virus-induced encephalomyelitis. *Ann Neurol* 1983, 13:426-433
29. Ludwin SK: Chronic demyelination inhibits remyelination in the central nervous system: An analysis of contributing factors. *Lab Invest* 1980, 43:382-387

### Acknowledgments

The expert technical assistance of Jannie Tong and the secretarial help of Lowella Rivero are greatly appreciated.